A Heterogeneous Hybrid Computational Electromagnetics Formulation Including Conduction Current Crossing the Domain Boundary

M A Mangoud, R A Abd-Alhameed and P S Excell

Telecommunications Research Centre, University of Bradford, Bradford, BD7 1DP, United Kingdom

Abstract - **A heterogeneous hybrid computational electromagnetics method is presented, which enables different parts of a problem space to be treated by different methods, thus enabling the most appropriate method to be used for each part. The method uses a standard frequency-domain Method of Moments program and a Finite-Difference Time-Domain program to compute the fields in the two regions. The interface between the two regions is a surface on which effective sources are defined by application of the Equivalence Principle. An extension to this permits conduction currents to cross the boundary between the different computational domains. Several validation cases are examined and the results compared with available data. The method is particularly suitable for simulation of the interaction of a mobile telephone with the human body in cases where the antenna has a complex shape and the chassis is in contact with the body tissue.**

Indexing terms: Computational electromagnetics, Hybrid methods, Method of Moments (MoM), Finite Difference Time Domain (FDTD)

I. INTRODUCTION

Certain problems, notably those involving coupling of a mobile telephone to human tissue, require use of the Finite-Difference Time-Domain (FDTD) method for one part of the problem and the Method of Moments (MoM) for another. These methods are commonly used in analysing complex electromagnetic problems, but they have significantly differing strengths and weaknesses. Usually, the frequency-domain MoM is used to analyse a structure up to a few wavelengths in size and it is particularly appropriate for simulation of wire structures, but it faces difficulties in handling substantial volumes of dielectric since the size of the interaction matrix becomes unmanageable when the number of quantisation elements exceeds a few tens of thousands. On the other hand, FDTD can handle substantial penetrable dielectric and partially-conducting structures (e.g. the human head), since each quantisation element interacts only with its nearest neighbours and not with the entire set of elements. The drawback of FDTD is in the modelling of curved structures of finite size, since the surfaces then become 'staircased' as a result of conformance to the rectangular quantisation grid: this poses particular problems when attempts are made to model the helical wire antennas that are now commonplace on mobile telephone handsets.

The basic hybridisation of the MoM and FDTD methods has been realized in the recent past and it has been extensively studied and tested in different applications [1-3]. The coupling between these methods is computed by using the Equivalence Principle theorem. In implementing this, the objects should not be physically connected, but separated by a small distance, sufficient to permit the equivalence-principle surface to be placed in isolation between them. This separation distance may be from infinity to a small fraction of a wavelength: 0.03λ has been found to give acceptable accuracy [2]. If the objects are physically connected and have some conductivity, for example, modelling a mobile handset in contact with the human head, a different treatment is required to allow the conduction current to cross the boundary between the two methods, applying a special treatment to ensure current continuity across the surface. Earlier work [1-3] is here extended for the case where the source region is subdivided such that conduction currents have to cross the dividing boundary, one part replaced by equivalent surface currents using the equivalence principle and computed by MoM; the other part handled with the use of direct impressed currents (suitable to couple with FDTD) [4].

Similar approaches have been proposed by others [5,6], although these use a time-domain version of MoM in the hybrid method. Time-domain MoM interfaces more naturally with FDTD, but it is not as well-developed as the frequency-domain version and hence the latter was adopted for the present work, applying a simple Fourier transform at the interface [1-4]. An industry-standard frequency-domain MoM program [7] was used in the work reported here, although it can easily be modified for use with any MoM program.

Coupling between the scatterer and source regions is calculated using the Reaction Theorem, with appropriate modifications to the MoM program to take account of the fact that the basis and weighting functions are not the same.

1054-4887 © 2001 ACES

II. THEORY OF THE MODIFIED HYBRID MoM/FDTD METHOD

Figure 1(a) shows two regions, one enclosing the source, the other enclosing a scatterer. To demonstrate the current-crossing treatment, the source region is subdivided into two sub-regions, *A* and *B*, as shown in Figure 1(b). The source region *B* and the scatterer region cannot be in contact, but the scatterer can be very close to, or attached to, the source region *A*.

In Figure 1(b) the surface S_c encloses the entire source region. The fields due to the induced currents from both source sub-regions *A* and *B* can be computed in order to evaluate the surface currents $\boldsymbol{J}_{si}$ and $\boldsymbol{M}_{si}$ over the modified closed surface S_{cl}:

$$\mathbf{M}_{si} = (\mathbf{E}(\mathbf{J}_A, \mathbf{M}_A) + \mathbf{E}(\mathbf{J}_B, \mathbf{M}_B)) \times \hat{\mathbf{n}} \tag{1}$$

$$\mathbf{J}_{si} = \hat{\mathbf{n}} \times (\mathbf{H}(\mathbf{J}_A, \mathbf{M}_A) + \mathbf{H}(\mathbf{J}_B, \mathbf{M}_B)) \tag{2}$$

where $\boldsymbol{J}_A$, $\boldsymbol{J}_B$, $\boldsymbol{M}_A$ and $\boldsymbol{M}_B$ are the electric and magnetic surface currents of source regions *A* and *B*; $\hat{n}$ is the unit vector normal to the surface S_{c1}.

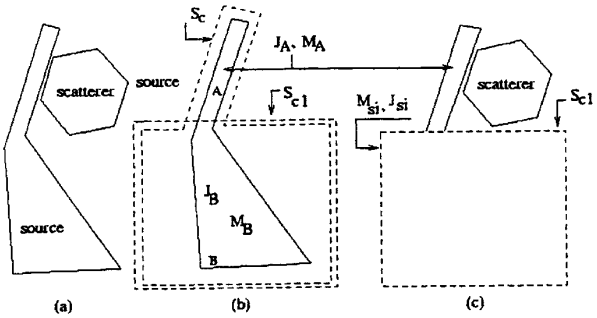

Figure 1 The basic geometry of the problem, with differing approaches to partitioning.

Now let the part of the surface S_c surrounding sub-region *A* be coincident with the surface of the conducting source structure within *A*. The currents on S_c then become the surface currents on the conductor which can be transferred to an FDTD model by treating them as impressed currents. The whole source region is then modelled using the FDTD method with impressed currents replacing sub-region *A* and a surface of equivalent currents replacing sub-region *B*. The impressed sources for a perfectly conducting surface (M_A = 0) considered in region *A* can be implemented in FDTD as follows:

$$\mathbf{E} = \mathbf{E}_{\mathrm{FDTD}} - \frac{\mathbf{J}_A}{(\varepsilon/\Delta t + \sigma/2)} \tag{3}$$

where E_{FDTD} represents the normal electric field finite difference updating equations, $\boldsymbol{J}_A$ is the electric surface current calculated using MoM, Δt is the time step, ε and σ are the permittivity and the conductivity of the surrounding medium. $\boldsymbol{J}_A$ is converted to a time domain waveform by extracting the magnitude and phase from the MoM results. At the same time, Huygens surface S_{cl} in region *B* is implemented with the modified total/scattered field formulation and using the evaluated surface currents $\boldsymbol{J}_{si}$ and $\boldsymbol{M}_{si}$ as described in [1], as follows:

$$\mathbf{E} = \mathbf{E}_{\mathrm{FDTD}} + \frac{\mathbf{J}_{\mathrm{si}}\big|_{Sc1}}{(\varepsilon/\Delta t + \sigma/2)} \tag{4}$$

$$\mathbf{H} = \mathbf{H}_{\mathrm{FDTD}} + \mathbf{M}_{\mathrm{si}}\big|_{Sc1}\frac{\Delta t}{\mu} \tag{5}$$

where J_{si} and M_{si} are the surface electric and magnetic currents, and where they have the suffix S_{cl} they are only the currents defined at the surface S_{cl}. μ is the permeability of the medium. The reaction on the source region *A*, R_A, due to the back-scattered fields from the scatterer is:

$$\mathbf{R}_A = <(\mathbf{E}_{\mathrm{free}} - \mathbf{E}_{\mathrm{scat}}), \mathbf{J}_{\mathrm{ts}}> = \int_{S_A} (\mathbf{E}_{\mathrm{free}} - \mathbf{E}_{\mathrm{scat}}) \bullet \mathbf{J}_{\mathrm{ts}} ds_A \tag{6}$$

where the symbols <> and "•" represent the inner product and the dot product respectively. The E_{free} and E_{scat} are the tangential electric fields on the surface bounding the region *A*, calculated in the FDTD domain, without and with the scatterer respectively. If these fields are assumed constant over each wire segment and the surface current testing functions are uniform over these segments then the above equation can be reduced to:

$$\mathbf{R}_A = (\mathbf{E}_{\mathrm{free}} - \mathbf{E}_{\mathrm{scat}}) \bullet \hat{\mathbf{i}}_{\mathrm{ts}} \Delta \tag{7}$$

where Δ is the FDTD cell size used and $\hat{i}_{ts}$ is a unit vector that represents the direction of the test current function $\mathbf{J}_{ts}$. The reaction on the source region *B*, R_B, i.e. the scattered field region, due to the back-scattered fields from the scatterer on the equivalent surface can be given as:

$$\mathbf{R}_B = <\mathbf{J}_{\mathrm{ts}}, \mathbf{E}_{\mathrm{ib}}> = \int_{S_B} \mathbf{J}_{\mathrm{ts}} \bullet \mathbf{E}_{\mathrm{ib}} ds_B \tag{8}$$

or

$$\mathbf{R}_B = <\mathbf{E}_{\mathrm{ts}}, \mathbf{J}_{\mathrm{ib}}> - <\mathbf{H}_{\mathrm{ts}}, \mathbf{M}_{\mathrm{ib}}> = \int_{S_{cl}^-} (\mathbf{E}_{\mathrm{ts}} \bullet \mathbf{J}_{\mathrm{ib}} - \mathbf{H}_{\mathrm{ts}} \bullet \mathbf{M}_{\mathrm{ib}}) ds_{cl}^- \tag{9}$$

where:

$$\mathbf{E}_{ib} = -j\omega\mathbf{A}(\mathbf{r}) - \nabla V(\mathbf{r}) - \frac{1}{\varepsilon}\nabla \times \mathbf{F}(\mathbf{r})$$

$$\mathbf{A}(\mathbf{r}) = \mu \int_{S_{c1}^-} \mathbf{J}_{ib} g(\mathbf{r},\mathbf{r}') ds_{c1}^-$$

$$V(\mathbf{r}) = \frac{-j}{\omega\varepsilon} \int_{S_{c1}^-} \nabla_s \bullet \mathbf{J}_{ib} g(\mathbf{r},\mathbf{r}') ds_{c1}^-$$

$$\mathbf{F}(\mathbf{r}) = \varepsilon \int_{S_{c1}^-} \mathbf{M}_{ib} g(\mathbf{r},\mathbf{r}') ds_{c1}^-$$

$$\mathbf{F}(\mathbf{r}) = \varepsilon \int_{S_{c1}^-} \mathbf{M}_{ib} g(\mathbf{r},\mathbf{r}') ds_{c1}^-$$

And $g(\mathbf{r},\mathbf{r}') = \dfrac{e^{-jk|\mathbf{r},\mathbf{r}'|}}{4\pi|\mathbf{r},\mathbf{r}'|}$ is the Green's function.

The vectors $\mathbf{r}$ and $\mathbf{r}'$ apply to the source and observation points respectively. S_B is the conducting surface area of the structure within region B. $\mathbf{J}_{ts}$ is the electric test function used on the wire or patch: it is usually a uniform pulse to account for the excitation voltage at the centre of the wire segment or patch in MoM formulations, such as NEC-2 [7]. $\mathbf{E}_{ts}$ and $\mathbf{H}_{ts}$ are the electric and magnetic fields respectively for the test function $\mathbf{J}_{ts}$. It should be noted that, in applying Eqn. (7), there is no magnetic test function specified in NEC-2 [7]. Since $\mathbf{E}_{ts}$ and $\mathbf{H}_{ts}$ can be obtained easily using NEC, after discarding the sinusoidal basis function terms, and assuming that the cell meshing used in FDTD is very small compared with the operating wavelength, Eqn. (9) can be reduced by ignoring the surface integral and evaluating the reaction on region B corresponding to the centre of the cell surface, as shown below:

$$\mathbf{R}_B = \sum_{n\ s_{c1}^-} (\mathbf{E}_{ts}(\mathbf{r},\mathbf{r}') \bullet \mathbf{J}_{ibn} - \mathbf{H}_{ts}(\mathbf{r},\mathbf{r}') \bullet \mathbf{M}_{ibn}) a_n \qquad (9)$$

where $\mathbf{r}'_n$ is the position vector of the centre of the cell surface and a_n is the surface area of the cell. Therefore $\mathbf{J}_{ibn}$ and $\mathbf{M}_{ibn}$ are considered to be the equivalent surface currents at the centre of the surface cell n. At the boundary of the impressed current source and the equivalent surface (S_{c1}) FDTD requires at least 2 to 3 cells of additional margin to recalculate the reaction in region B, as seen from Fig. 1(b). When the reactions have been obtained, the new currents can be computed and the method can be repeated until the steady state is reached.

III. SIMULATIONS AND RESULTS

Near fields and input impedance are taken to be convenient but rigorous validation parameters for the following examples:

1. A perfectly electrically conducting (PEC) half-wavelength dipole with radius 0.001m, in free space, was first considered. The chosen simulation frequency was 961MHz, with wavelength equal to 0.31212m and the FDTD cell size equal to 0.00306m. Thus the dipole was considered as 51 cells in the z direction. The equivalent surface treatment was arbitrarily chosen to enclose 19.6% (0.098λ, equal to 10 cells) of the length of the dipole to be modelled using MoM, whereas the rest of the dipole (41 cells) was replaced by the impressed currents inside the FDTD problem space (as in Figure 2(a), without the scatterer). The free space electric field on a line parallel to the dipole at a transverse distance of 0.0346λ was examined, as shown in Figure 3. The results of the proposed current crossing technique are in good agreement with those from the hybrid MoM/FDTD method (with Huygens surface surrounding the full dipole) and the pure MoM NEC programs.

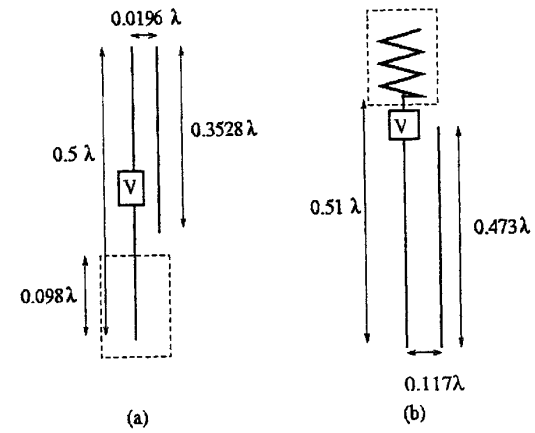

Figure 2 The geometry of the examples 2 and 3.

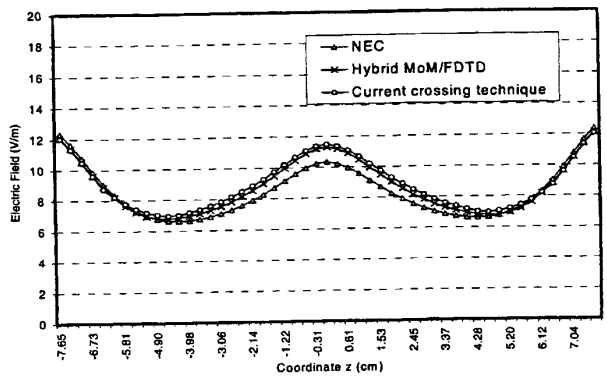

Figure 3 Comparison between the computed near electric fields of a dipole in free space (Example1)

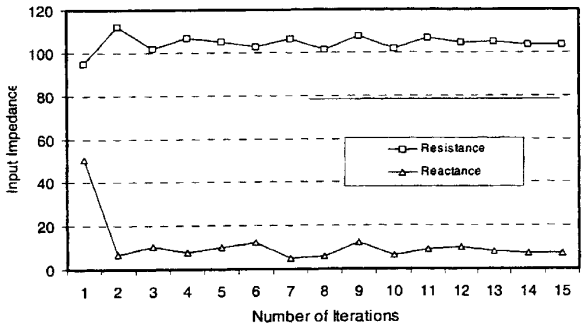

Figure 4 Input impedance of the source dipole with scatterer of Example 2, versus number of iterations, for current-crossing hybrid treatment.

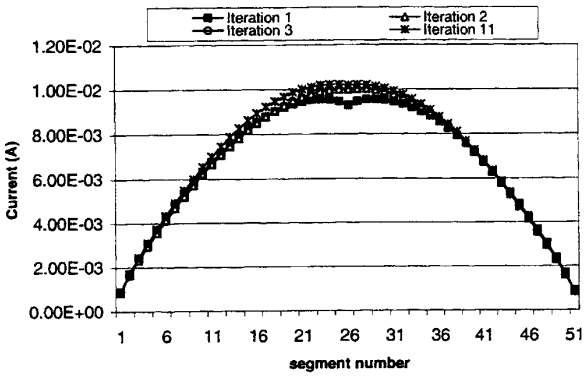

Figure 5 Magnitude of the current in the source dipole with scatterer of Example 2, along the dipole length for different numbers of iterations.

2. A wire scatterer was introduced adjacent to the half-wavelength dipole of the previous example, in the form of a PEC rod of length 0.3528λ (36 cells) and radius 0.001m, parallel to the source dipole at a distance 0.0196λ, equivalent to two FDTD cells, (see Figure 2(a)). The scatterer was located in the region of the impressed current source. The dipole here was modelled using the current crossing technique, using a Huygens surface to enclose 19.6% (0.098λ) of the length of the dipole. The impressed currents were used for the rest of the dipole inside the FDTD part of the program. The input impedance of the source dipole versus the number of iterations is shown in Figure 4. The results converge to Z = 103+j8 Ω after 15 iterations. This is in good agreement with the result from a uniform MoM treatment (NEC)[7], which gave Z = 110+j10 Ω. Figure 5 shows the continuity of the current that crosses the domain boundary, displayed for iterations Nos. 1, 2, 3 and 11 for this example. It clearly shows the continuity of the current crossing segment No. 11 where the connection to the Huygens surface is placed: virtually no distortion or asymmetry is visible.

3. In this example the source region contains a dipole with total conductor length 1.0λ and radius 0.001m. The working frequency was doubled to become 1922MHz, corresponding to a wavelength of 0.156m. Similarly to the previous example, a cell size of 0.00306m was used. As illustrated in Figure 2(b), one of dipole arms is coiled into a helix with three turns, having coil radius and pitch both equal to 0.004m. The scatterer is a wire of length 0.473λ (24 cells) and radius 0.001m. The scatterer and the source are separated by 0.1176λ (6 cells). The equivalent surface encloses the helix region (treated by MoM) while the impressed current treatment (FDTD region) is used for the other arm of the dipole. The input impedance versus the number of iterations is shown in Figure 6: convergence occurs within 10 iterations, although the results are close to convergence even after only four iterations. The results converge to Z = 420-j190 Ω which is in good agreement with a non-hybrid NEC-only treatment: Z = 462-j220 Ω.

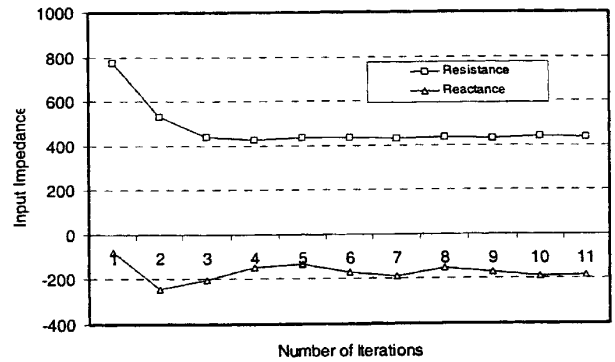

Figure 6 Input impedance of the semi-helical dipole with scatterer of Example 3, versus number of iterations, for hybrid current-crossing treatments.

The accuracy of this proposed modified hybrid method is demonstrated in Figures 7 and 8. These show the computed near field magnitude distribution contours for the above examples, showing the conduction current crossing domain boundaries for both the dipole and the helix-dipole in free space and with a wire scatterer. In the free space simulation of Figure 7(a) the symmetric patterns of the half-wavelength dipole in the total field region outside the Huygens surface can be observed. Figure 8(a) shows a reasonable pattern with expected asymmetry for the helix-dipole combination of length 1.0λ, with a minimum near field value around the middle of the straight half of the dipole. In both Figures 7(a) and 8(a), the near field values (scattered field) inside the Huygens surface are close to zero, indicating very little scattered field, as expected. Also, it is noticed that the boundary area of connection between the wire and the virtual surface shows very little disruption to the fields in the scattered region, hence indicating that the proposed current crossing treatment is implemented successfully. Figures 7(b) and 8(b) illustrate near field contours in the presence of

scatterers. It can be noted that more back-scattered field is observed inside the Huygens surface for the helix-dipole as compared with the dipole. This is because of the closer proximity of the scatterer to the crossing boundary in the helix-dipole case.

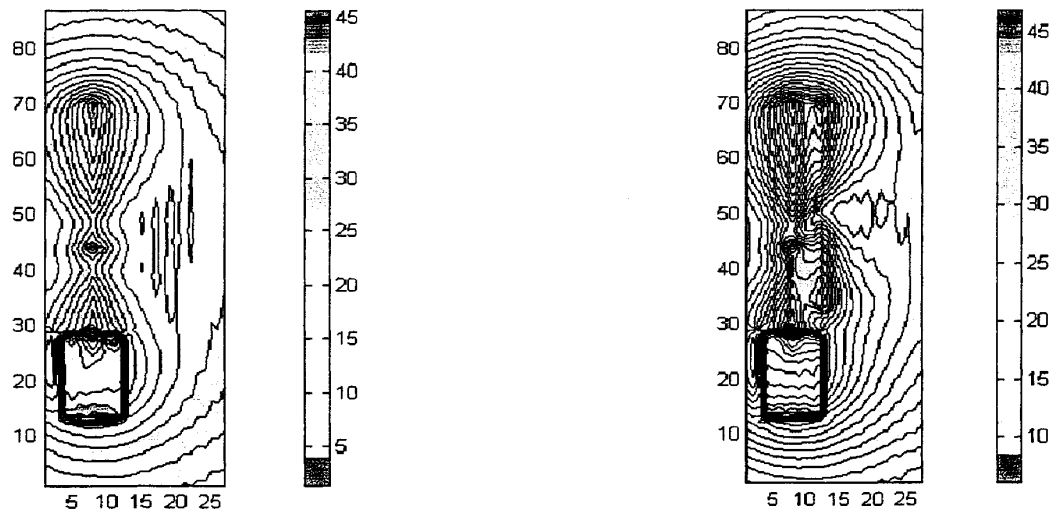

(a) (b)

Figure 7 Vertical slice cut for computed near electric field magnitude distribution contours (in dBV/m) for the example 2

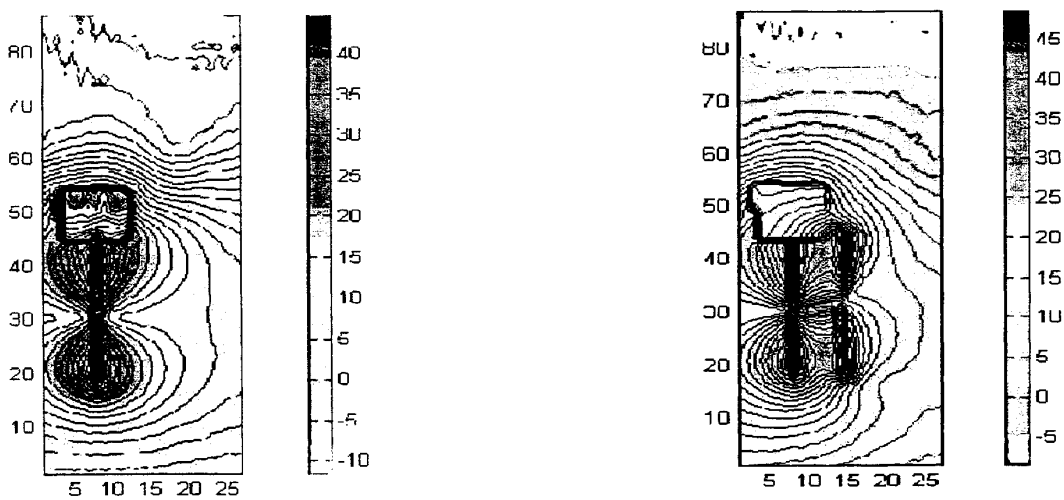

(a) (b).

Figure 8 Near field contours on the central y-z plane for Example 3: (a) without the scatterer; (b) with the scatterer.

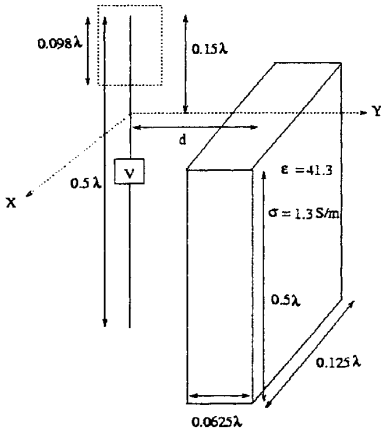

Figure 9 The geometry of the problem for Example 4.

4. In this case the scatterer region is taken to be a sheet of lossy dielectric simulating human tissue. The sheet dimensions are 0.125λ x 0.0625λ x 0.5λ, with a relative permittivity of 41.3 and a conductivity of 1.3 Sm^{-1}, as presented in Fig. 9. The input impedance versus the number of iterations required to reach steady state solution, for three different distances, is shown in Fig. 10. The results are in excellent agreement with the data in [8]. The far field pattern for two different planes using the current crossing hybrid MoM/FDTD technique is shown in Fig. 11.

IV. CONCLUSIONS

A hybrid method using MoM and FDTD has been successfully implemented using two separate current regions for the source, applying the two different methods in each and allowing conduction current flow across the boundary between them. The method is capable of handling problems even when the scatterer is attached to, or very close to, part of the source region. Good convergent results are obtained after a few iterations and the results are in good agreement with the available data.

Such hybrid methods are particularly appropriate for simulation of the interaction of a mobile telephone with the human body since the details of the telephone can be simulated quasi-conformally by MoM, while retaining the more traditional FDTD treatment for the body tissue. The basic hybrid methods do not permit current flow across the boundary separating the two domains, but the treatment presented here has demonstrated a method to achieve this. This technique has particularly important applications in cases where the telephone antenna has a complex shape and the chassis is in contact with the body tissue.

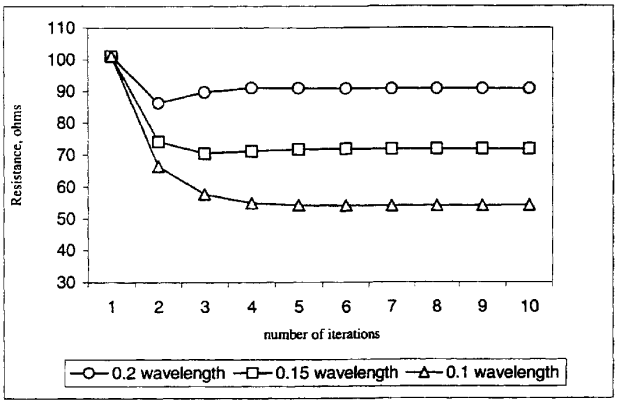

(a)

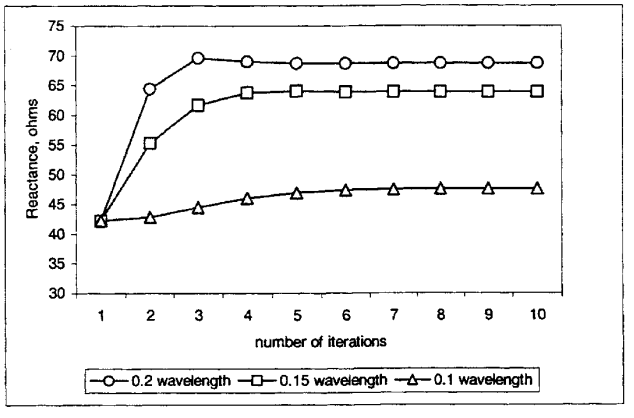

(b)

Figure 10 The input resistance and reactance of the source dipole in Example 4, for three different distances from the dielectric.

REFERENCES

1. Abd-Alhameed, R.A., Excell, P.S., Vaul, J.A. and Mangoud, M.A.: 'Hybrid treatment for electromagnetic field computation in multiple regions', *Electronics Letters*, Vol. 34, No. 20, pp. 1925-1926, 1998.

2. Mangoud, M.A., Abd-Alhameed, R.A. and Excell, P.S.: 'Simulation of human interaction with mobile telephones using hybrid techniques over coupled domains', *IEEE Trans. on Microwave Theory and Techniques*, Vol. 48, No. 11, pp. 2014-2021, 2000.

3. Abd-Alhameed, R.A., Mangoud, M.A. and Excell, P.S.: 'Investigation of reduced SAR personal communications handset using hybrid MoM/FDTD technique', Archiv für Elektronik und Übertragungstechnik, Vol. 54, No. 3, pp. 147-154, 2000.

4. Mangoud, M.A., Abd-Alhameed, R.A., Excell, P.S., and Vaul, J.A.: 'Conduction current crossing domain boundaries in a heterogeneous hybrid computational electromagnetics formulation', *Electronics Letters*, Vol. 35, No. 21, pp. 1786-1788, 1999.

5. Cerri, G., Chiarandini, S., Russo, P. and Schiavoni, A.: 'Electromagnetic coupling between arbitrarily bent wires and scatterers analysed by a hybrid MoMTD/FDTD approach', IEE Proc., Vol. , No. , pp. 261-, 2000.

6. Lautru, D., Wiart, J., Tabbara, W. and Mittra R.: 'A MoMTD/FDTD hybrid method to calculate the SAR induced by a base station antenna', *IEEE AP Society International Symposium*, Salt Lake City, Utah, Vol. 2, pp. 757-760, 2000.

7. Burke, G.J., and Poggio, A.J.: 'Numerical electromagnetics code (NEC): method of moments', US Naval Ocean Systems Center, San Diego, Rep. No. TD116, 1981.

8. Abd-Alhameed, R.A. and Excell, P.S.: 'Analysis of dielectrically-loaded wire, strip and patch antennas, using method of moments', Proc. IEE Conf. on Computation in Electromagnetics, Bath University, pp 306-311, 1996.

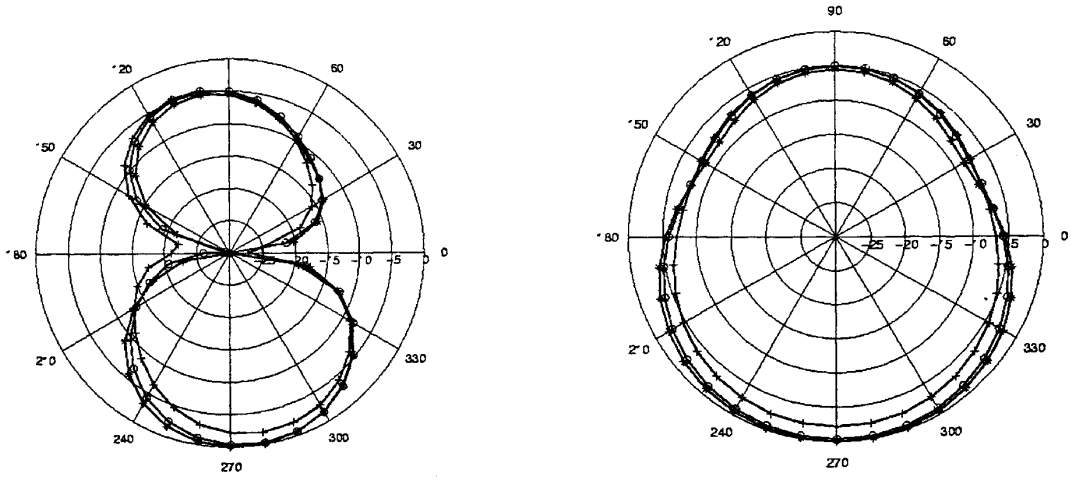

Figure 11 The far-field E_θ component for Example 4, for two different cuts: (a) vertical cut at $\phi = 90°$; (b) horizontal cut at $\theta = 90°$. ('+++' d = 0.1λ, 'ooo' d = 0.15λ, '***' d = 0.2λ)